NUMERICAL COMPUTATION OF DIFFERENT ASPECTS OF 26 DECEMBER 2004 TSUNAMI ALONG THE PENANG ISLAND USING A CYLINDRICAL POLAR MODEL

[1]Md. Fazlul. Karim, [2]Gauranga Deb Roy, [3]Ahmad Izani Md. Ismail
[1]Permanent position: Dept. of Sc. Math. & Tech. education, IER, Dhaka University, Dhaka 1000, Bangladesh
[2]Permanent position: Dept. of Mathematics & Natural Sciences, BRAC University, Dhaka 1212, Bangladesh
[3]School of Mathematical Sciences, University Sains Malaysia, 11800 Pulau Pinang
e-mail: [1]mdfazlulk@yahoo.com, [2]gdroy@gononet.com, [3]izani@cs.usm.my

Abstract. *The tsunami of December 26, 2004 was devastating in its effect on the island of Penang. A numerical model based on the linear shallow-water equations in cylindrical polar coordinate system was discussed and the results presented in a previous study (Roy and Izani, 2005). In this study we investigate the effects of using a more refined grid on the wave height distribution along the coastline of Penang. We also study the effect of changing the orientation of the source. Our studies show that the more refined grid is capable of generating wave heights in good agreement with observed data without excessively increasing the computation time. It is also found that orientation of the source have a significant effect on the wave heights.*

1 Introduction

The west coast of peninsular Malaysia including Penang is vulnerable to the effects of seismic sea waves, or tsunamis, generated along the active subduction zone of Sumatra and that was demonstrated on December 26,2004. The devastating mega thrust earthquake (Indonesia/ Nicobar/ Andaman/ Sumatra Earthquake) occurred on Sunday, December 26, 2004. The earthquake also triggered a giant tsunami that propagated throughout the Indian Ocean and caused extreme inundation and extensive damage along the coasts of 12 countries surrounding the Indian Ocean. It was reported that 68 people died in Penang state, Malaysia (AFP, 2005) out of which 57 were from Penang Island (Yasin, 2005) and the remaining from the mainland part of the Penang.

Forecasting of any future earthquake is not possible at present and hence the time of arrival of the next large tsunami is unknown. It is certain, however, that these events will continue to occur and that the risk to lives and property is very real and should not be ignored. So it is necessary to have an estimate of the largest waves that can be expected to arrive towards Penang Island. It is now possible to simulate tsunami propagation and inland inundation by numerically solving the appropriate mathematical equations and boundary conditions. This approach allows complete flexibility in specifying tsunami source regions and generation mechanisms, as well as treating the complex topography and bathymetry of the coastal waterways.

A tsunami is a long wave generated by ocean bottom motion during an earthquake with wave length of about 200 to 350 km. Tsunamis are generated due to disturbances of free surface caused not only by seismic fault motion, but also by landslides and volcanic eruptions (Imamura and Imteaz,1995). Although the wave amplitude is moderate in deep waters (e.g. 0.5 to 1 m), the tsunami wave slows down and the wave height increases near the shoreline until it breaks. The wave run-up height might reach several meters above the mean sea level and cause significant damage.

Many works on generation, propagation and run-up of tsunami have been done so far. Titov (1997), Titov and Gonzalez (1997) developed the MOST (Method of Splitting Tsunami) Model that is capable of generation of tsunami by an earthquake, transoceanic propagation, and inundation of dry land; the generation process is based on elastic deformation theory (Okada, 1985).

A non-linear numerical model for stratified tsunami waves was developed by Imteaz et al. (2001). Recently Kowalik et al. (2005) has developed a new model for the global tsunami computation. This model was applied to simulate the tsunami of 26 December 2004 between 80^o S and 69^o N. They used the spherical polar shallow water model incorporating a very fine mesh resolution of 1 minute with about 200 million grid points.

Roy et al. (1999) developed a polar coordinate shallow water model to compute tide and surge due to tropical storms along the coast of Bangladesh. Haque et al.(2003) improved the model of Roy et al. (1999) for achieving finer resolution in the numerical scheme along the coastal belt of Bangladesh. Following the approach of Roy et al. (1999) and Haque et al. (2003), Roy and Izani (2005) developed a Cylindrical Polar model to simulate tsunami wave propagation and to estimate water level and other related aspects along the coast of Penang Island associated with 26 December 2004 tsunami source at Sumatra.

In the present study, the model of Roy and Izani (2005) has been used, with finer grid resolution, to simulate the propagation of 26 December 2004 tsunami wave towards the Penang Island and to estimate the water levels along its coastal belts (Fig.1). The model has also been applied to compute other related aspects of tsunami surrounding the Penang Island. In particular we study the effects of different orientations of the tsunami source.

2 Mathematical formulation

2.1. Governing Equations

To simulate the tsunami wave propagation, the vertically integrated shallow water equations, given by Roy et al. (1999) are used. They used a system of Cylindrical Polar coordinates in which the origin, O, is at the undisturbed level of the sea surface (the $r\theta$-plane) and OZ is directed vertically upwards. The displaced position of the free surface is $z = \zeta(r, \theta, t)$ and the position of the sea floor is $z = -h(r, \theta)$ so that the total depth of the fluid layer is $\zeta + h$. The equations are,

$$\frac{\partial \zeta}{\partial t} + \frac{1}{r}\frac{\partial}{\partial r}\left[r(\zeta + h)v_r\right] + \frac{1}{r}\frac{\partial}{\partial \theta}\left[(\zeta + h)v_\theta\right] = 0 \tag{1}$$

$$\frac{\partial v_r}{\partial t} - fv_\theta = -g\frac{\partial \zeta}{\partial r} - \frac{F_r}{\rho(\zeta + h)} \tag{2}$$

$$\frac{\partial v_\theta}{\partial t} + fv_r = -\frac{g}{r}\frac{\partial \zeta}{\partial \theta} - \frac{F_\theta}{\rho(\zeta + h)} \tag{3}$$

where

v_r = radial component of velocity of the sea water
v_θ = tangential component of velocity of the sea water
F_r = radial component of frictional resistance at the sea bed
F_θ = tangential component of frictional resistance at the sea bed
f = Coriolis parameter $= 2\Omega\sin\varphi$
Ω = angular speed of the earth
φ = latitude of the location
g = acceleration due to gravity

The parameterizations of F_r and F_θ are done by conventional quadratic law:

$$F_r = \rho\, C_f v_r \sqrt{{v_r}^2 + {v_\theta}^2} \quad \text{and} \quad F_\theta = \rho\, C_f v_\theta \sqrt{{v_r}^2 + {v_\theta}^2} \tag{4}$$

where ρ is the sea water density and C_f is the friction coefficient.

2.2. Boundary conditions

For a closed boundary the normal component of velocity is considered as zero. The radiation type of boundary conditions are used for open boundaries which allow the disturbance created within the analysis area to go out of the area. The model area is bounded by the straight lines $\theta = 0$ and $\theta = \Theta$ through the pole O and the circular arc $r = R$ with center at O.

Following Roy et.al (1999) northern, southern and western open sea boundary conditions are respectively given by

$$v_\theta + \sqrt{(g/h)}\ \zeta = 0 \quad \text{along } \theta = 0 \tag{5}$$

$$v_\theta - \sqrt{(g/h)}\ \zeta = 0 \quad \text{along } \theta = \Theta \tag{6}$$

$$v_r - \sqrt{(g/h)}\ \zeta = 0 \quad \text{along } r = R \tag{7}$$

2.3 Transformation to stretch along radial direction

To incorporate the bending of the coastline and the offshore islands, the mesh size should be small near the coastal belt, whereas this is unnecessary away from the coast. The Polar coordinate system ensures the finer mesh along tangential direction. For uniform grid size $\Delta\theta$ in the tangential direction, the arc distance between any two consecutive radial straight grid lines decreases towards the pole and increases away from the pole. Thus the arc distance increases as we move away from the coast although the grid size $\Delta\theta$ is uniform.

To perform the stretching along radial direction, so that the physical mesh becomes finer near the coast and coarser in deep sea, according to Haque et al. (2003), the following transformation is used:

$$\eta = c \ln\left(1 + \frac{r}{r_0}\right) \quad \text{and} \quad \theta = \theta \tag{8}$$

where r_0 is of the order of total radial distance of the analysis area and c is a scale factor. From this transformation we obtain a relationship between Δr and $\Delta\eta$ which is as follows:

$$\Delta r = \frac{r + r_0}{c} \Delta\eta \tag{9}$$

This relation shows that keeping constant value of $\Delta\eta$, we can generate variable Δr, which increases with increase of r, so that we obtain uneven resolution (fine to coarser) in the radial direction in the physical domain while in the computational domain ($\eta\theta$ domain) the resolution remains uniform.

Using the above transformation equations (1) – (3) transform to

$$\frac{\partial\zeta}{\partial t} + \frac{ce^{-\eta/c}}{r_0\,(e^{\eta/c}-1)} \frac{\partial}{\partial\eta}\left\{(\zeta + h)\ (e^{\eta/c}-1)\, v_r\right\} + \frac{1}{r_0\,(e^{\eta/c}-1)} \frac{\partial}{\partial\theta}\left\{(\zeta + h)\, v_\theta\right\} = 0 \tag{10}$$

$$\frac{\partial v_r}{\partial t} - f v_\theta = -\frac{gce^{-\eta/c}}{r_0} \frac{\partial\zeta}{\partial\eta} - \frac{C_f v_r \sqrt{{v_r}^2 + {v_\theta}^2}}{(\zeta + h)} \tag{11}$$

$$\frac{\partial v_\theta}{\partial t} + f v_r = -\frac{g}{r_0\,(e^{\eta/c}-1)} \frac{\partial\zeta}{\partial\theta} - \frac{C_f v_\theta \sqrt{{v_r}^2 + {v_\theta}^2}}{(\zeta + h)} \tag{12}$$

The boundary conditions (5)-(7) do not change due to the transformation.

2.4 Numerical Grid Generation

In this study, a shallow water model in Cylindrical Polar Coordinate system is used where the Pole is placed on the mainland of Penang at O (5^o 22.5′N, 100^o 30′ E) and the model area extends from Penang to the west of Sumatra and includes the Malacca straits. In the physical domain the curvilinear grid system is generated

through the intersection of a pencil of straight lines through O given by θ = *constant* and a set of concentric circles, with centre as O, given by r = *constant*. The uniform angle between any two successive straight lines is taken as $\Delta\theta = 0.3333^0$, whereas the distance between two successive circular grid lines, Δr, increases as we proceed towards the open sea.
After the transformation, given by Eq. (8), both $\Delta\theta$ and $\Delta\eta$ become uniform. In the transformed domain, i.e., in η-θ plane, the discrete grid points (η_i, θ_j) are defined by

$\eta_i = (i-1)\,\Delta\eta; \quad i = 1, 2, 3, \ldots, m$
$\theta_j = (j-1)\,\Delta\theta; \quad j = 1, 2, 3, \ldots, n$

where m = 778 and n = 277 also $\Delta\theta$ =0.3333^o and $\Delta\eta$ = 1/1077, so that in the computational domain η ranges from 0 to 777/1077. Although $\Delta\eta$ is taken as a constant, Δr increase with r according to the Eq. (9) and varies from 0.5 km to 1.0 km. Thus we obtain a finer mesh near the coast and gradually coarser mesh in the deep sea.

The sequence of time is given by

$$t_k = k\Delta t\,;\; k = 1, 2, 3, \ldots \tag{13}$$

Although, in the physical domain n grid lines meet at the Pole, in the computational domain this point is considered as n distinct grid points which are generated automatically. Since the pole is considered at the land, where no computation is done, there will be no problem of instability during numerical computation.
In the computational domain a staggered grid system is used where there are three distinct types of computational points (Fig.2). A single parameter (dependent variable) is computed at any one of these three types of points rather than at every point so that the CPU time is reduced. Moreover, staggered grid system is favorable in filtering out sub-grid scale oscillations and thus ensures numerical stability. Three types of points (η_i, θ_j) are defined as follows: if i is even and j is odd, the point is a ζ-point at which ζ is computed. If i is odd and j is odd, the point is a v_r-point at which v_r is computed and if i is even and j is even then the point is a v_θ-point where v_θ is computed. We choose m as even so that at the open sea boundary there are ζ-points and v_θ-points. Also n is chosen as odd so that there are only ζ-points and v_r-points at $\theta = 0^o$ and $\theta = \Theta = 92^o$. The coastal boundary is approximated either along the nearest odd tangential grid line, so that there are only v_r-points on this segment or along the nearest even radial grid line, so that there are only v_θ-points on this segment. Thus the boundary of the coast is represented by such a stair step that at each segment (tangential or radial) there exists only that component of velocity which is normal to the segment. This is done in order to ensure the vanishing of the normal component of velocity at the boundary in the numerical scheme.

2.5 Numerical Scheme

The governing equations (10) – (12) and the boundary conditions (5) – (7) are discretised by finite-differences (forward in time and central in space) and are solved by a conditionally stable semi-implicit method. For numerical stability, the velocity components in Eqs.(11) and (12) are incorporated in a semi-implicit manner. For example, in the last term of Eq.(11) the time discretisation of $v_r\sqrt{\left(v_r^2 + v_\theta^2\right)}$ is done as $v_r^{\,k+1}\sqrt{\left(v_r^2 + v_\theta^2\right)^k}$ where the superscripts k and $k+1$ denote the values of v_r at present and advanced time steps respectively. Moreover, the CFL criterion has been followed in order to ensure the stability of the numerical scheme. Along the closed boundary, the normal component of the velocity is considered as zero, and this is easily achieved through appropriate stair step representation as mentioned earlier. The time step is taken as 5 seconds that ensures stability of the numerical scheme. In the solution process, the value of the friction coefficient C_f is taken as uniform throughout the physical domain, which is 0.0033.

3 Initial condition (Tsunami source generation)

The devastating mega thrust earthquake (Indonesia/ Nicobar/ Andaman/ Sumatra Earthquake) of December 26, 2004, occurred on Sunday, December 26, 2004 at 00:58:53 GMT with Mw = 9.0 and Epicenter at 3.32° N, 95.85° E (USGS) or 3.09 N, 94.26E southwest Banda Aceh in Northern Sumatra (Borrero, 2005). The earthquake occurred on the interface of the India and Burma plates and was caused by the release of stresses that developed as the India plate subducts beneath the overriding Burma plate. A detailed description of the estimation, based on Okada (1985), of the extent of earthquake rapture (92°E to 97°E and 2°N to 10°N) along

with the maximum uplift (507 cm) and subsidence (474 cm) of the seabed has been reported in Kowalik et al. (2005). According to this estimation, the source is elongated from south-east to north-west with uplift to subsidence from west to east, so that relative to the west coast of Peninsular Malaysia the tsunami source is in the form of subsidence to uplift. Following Kowalik et al. (2005), a source, of the same extent with maximum uplift of 5 m and maximum down-drop of 4.75 m of the sea surface, is assigned as the initial condition. Fig. 3 shows the contour form of the source and Fig.4 shows the vertical cross-section of the source along 121st radial grid line. Other than source region the initial sea surface elevations are taken as zero everywhere. Also the initial radial and tangential components of velocity are taken as zero throughout the domain.

4 Numerical results

The effects of tsunami of December 26, 2004, having its source at Sumatra and for two other orientations, along the coast of Penang Island are investigated. Numerical simulation of this potential tsunami is performed in the framework of linear shallow-water equations in cylindrical polar coordinate system.

4.1 Propagation of tsunami towards Penang Island

The propagation of the disturbance along the 121st radial gridline starting from the western open boundary to the coast of Penang Island (778th to 67th grid points) is shown in fig.5. This shows the disturbance pattern at initial time, 30 min, 60 min, 120 min and 194 min (time of maximum water level near the west coast of Penang Island) along the 121st grid line. It is seen that the tsunami wave reaches the grid locations 530, 325 and 160 at approximately 30 min, 60 min, and 120 min respectively. Thus the computation shows that the tsunami gradually propagates towards Penang Island and attains a maximum of 3.4 m near the west coast at 194 min. Fig.6 shows the contour plot of propagation of tsunami in minutes for attaining +0.1 m sea level rise at each grid point. Thus considering the 0.1 m sea level rise as the arrival of tsunami, it is seen that after introducing the source the disturbance propagates gradually towards the Penang Island (Located at the top of fig.6) and reaches the west coast approximately 200 min after the generation of the source near Sumatra.

4.2. Computed water levels along Penang Island

The water levels at different locations of the coastal belt of Penang Island are stored at an interval of 60 seconds. Fig.7 describes the computed time histories of water levels at four locations on the north and west coasts of Penang Island. The maximum amplitude at Batu Ferringhi is approximately 2.6 m (Fig. 7a). It is seen that at approximately 2.75 hrs after the generation of tsunami at the source, the water level starts decreasing instead of increasing (withdrawal of water) and reaches level of -1.2 m. Then the water level increases continuously to reach a level of 2.6 m at 2 hrs 45 min before going down again. The reason for the withdrawal of water before arrival of tsunami surge has been discussed in Roy and Izani (2005). The computed water level at Tanjung Tokong, located east of Batu Ferringhi shows the same pattern as that of Batu Ferringhi with the maximum level of approximately 0.8 m (Fig.7b). At Pantai Aceh and near Pasir Panjang the maximum elevations are found to be 3.1 m and 3.0 m respectively (Figs. 7c & 7d). The computed results show that the west coast of Penang Island is vulnerable to a stronger tsunami surge. The computed results show that, the more refined grid is capable of generating wave heights in good agreement with observed data without excessively increasing the computation time compared to that of Roy and Izani (2005).

4.3. Surge Sensitivity due to source orientation

In order to investigate the effect of the sources with same intensity but different orientations, simulations have been carried out for three different orientations of the source which are as follows: the original source, the source elongated along the circular grid lines and the source elongated along radial grid lines; henceforth will be abbreviated as OS, CS and RS respectively. The maximum water levels along four coastal belts associated with the OS, CS and RS are presented in Fig. 8. There is over all increase of the maximum water level along every coast due to CS with highest intensity along the west coast. As much as 5 m surge was attained at the west coast due to CS. On the other hand, lowest intensity was attained at every coast due to RS. The results indicate that response along the west coast is more sensitive to the orientations of the source and the Penang Island will be more affected due to CS. This means that if the orientation of the source is such that Penang Island is towards the perpendicular direction to the elongation of the source, the island may be more affected by tsunami surge. Hence orientation of a tsunami source has a significant role on the surge intensity along the coastal belt.

Finally, a post tsunami survey report on run-up heights at different locations of Penang Island, along with the computed water levels, is shown in Table 1. It may be noted that the computed water level cannot be compared with observed run-up height data, although keeping all other conditions the same, the run-up height is directly proportional to the water level at the shore line. For the same water level at two different locations the run-up height will in general be different because of the different pattern of the onshore region. For example two locations of Pasir Panjang are very close to each other. The computed water levels are also same (about 3.3 m); but the run-up heights are 8.5 m and 4.2 m respectively. According to the survey report, at the first location, the tsunami wave jumped over a slope wall and the roof of the house behind; whereas in the second location the inundation was blocked by a hill. However, a consistency between the computed water level and the run-up height at each location may be observed from the table except at Tanjong Tokong where run-up height is 3.65 against 0.994 m water level.

Conclusions

Numerical simulation of the tsunami propagation from the source is performed in the framework of the linear shallow-water equations in cylindrical polar coordinates. Numerical simulation of the tsunami propagation for several orientations of the source has also been performed. This analysis demonstrates that the water level due to the tsunami wave from the source at Sumatra towards the Penang Island is in reasonable agreement with data of observations. According to the results for orientations of the source reported here, such prediction could be significant for amplitude estimation for different orientations of the source.

The numerical model for simulating the water level due to 26 December, 2004 tsunami presented here can be applied easily to model to any localized coastal region where a tsunami hazards exists, to help provide an effective warning system.

Acknowledgements

This research is supported by a short-term grant of Universiti Sains Malaysia and the authors acknowledge the support of the USM short-term grant. The first and second authors wish to thank USM authority for allowing them to serve as faculty members in the School of Mathematical Sciences. The authors would like to thank Prof S. B. Yoon, Hanayng University, Korea for providing the survey data on the tsunami run-up height along the coastal belt of Penang Island.

References

1. AFP, (2005), Death toll in Asian Tsunami Disaster
http://story.news.yahoo.com/news?tmpl=story2&u=/afp/20050305/wl_asia_afp/asiaquaketoll
Borrero,j.(2005), " Learning from earthquakes, The Great Sumatra Earthquake and Indian Ocean Tsunami December 26, 2004, Field Survey of Northern Sumatr," Report# 1EERI, Special Earthquake report, March 2005.

2. Haque, M.N.; Miah, S., Roy, G.D.;(2003): A Cylindrical Polar Coordinate Model with Radial Stretching for the coast of Bangladesh, Proc. Int. Conf. App. Math. & Math. Phy. (ICAMMP), Shahjalal Univ. of Sc. & Tech. Sylhet, Bangladesh, pp 77-87.

3. Imamura. F.; Imteaz. M.A.;(1995):Long Waves in Two Layers: Governing Equations and Numerical Model, Sc. of Tsunami Hazards, Vol.13, No.1, pp.3-24.

4. Imteaz. A. M.; Imamura. F.;(2001): A Non-Linear Numerical Model For Stratified Tsunami Waves and its Application.

5. Kowalik. Z.; Knight. W.; Logan. T.; (2005) Whitmore. P.:Numerical Modeling of The Global Tsunami, Sc. of Tsunami Hazards, Vol.2, No.1, pp.40.

6. Okeda, Y. (1985): Surface Deformation due to Shear and Tensile Faults in a Half Space; Bull. Seism. Soc. Am., 75: 1135-1154.

7. Roy, G. D. A. Izani Md. Ismail (2005): Numerical Modelling of Tsunami along the Coastal Belt of Penang using a Polar Coordinate Shallow Water Model; *Dyn. Atm. & Oceans* (communicated)

8. Roy, G.D.; Humayun Kabir, A.B.;Mandal, M.M.; Haque, M.Z.(1999): Polar Coordinate Shallow Water storm surge model for the coast of Bangladesh, Dyn. Atms. Ocean, 29, 397-413.

9. Titov,V.V., Gonzalez, F.I. (1997): Implementation and Testing of the Method of Spliting Tsunami (MOST) Model; NOAA Technical Memorandum ERL, PMEL -112, Contribution No. 1927 from NOAA/Pacific Marine Environmental Laboratory: pp 11.

10. Yasin, Z., 2005.The Tsunami Timeline. The School of Biological Science Bulletin, University Sains Malaysia, Vol VIII, 26

Table 1. Observed run-up heights and computed water levels at different locations of Penang Island

Location name	Latitude	Longitude	Run-up height (m)	Computed water level (m)
1	2	3	4	5
Batu Ferringhi (Taluk Bayu)	5° 28.26′	100° 14.63′	3.46	2.804
Batu Ferringhi (Miami beach)	5° 28.67′	100° 16.07′	4.00	2.584
Tanjug Tokong	5° 27.62′	100° 18.48′	3.65	0.994
Tanjug Tokong	5° 27.70′	100° 18.5′	2.61	0.994
Pasir Panjang	5° 18′	100° 11.09′	8.50	3.292
Pasir Panjang	5° 17.99′	100° 11.1′	4.20	3.292
Pulau Betung	5° 18.4′	100° 11.66′	3.23	2.851
Sungai Burung	5° 20.35′	100° 11.79′	4.28	2.857
Tanjong Bunge	5° 28.21′	100° 16.66′	2.31	1.109
Tanjong Bunge	5° 28.2′	100° 16.65′	2.94	1.269

Source: This survey is conducted by a team headed by Prof. S. B. Yoon, Hanayng University, Korea.

.

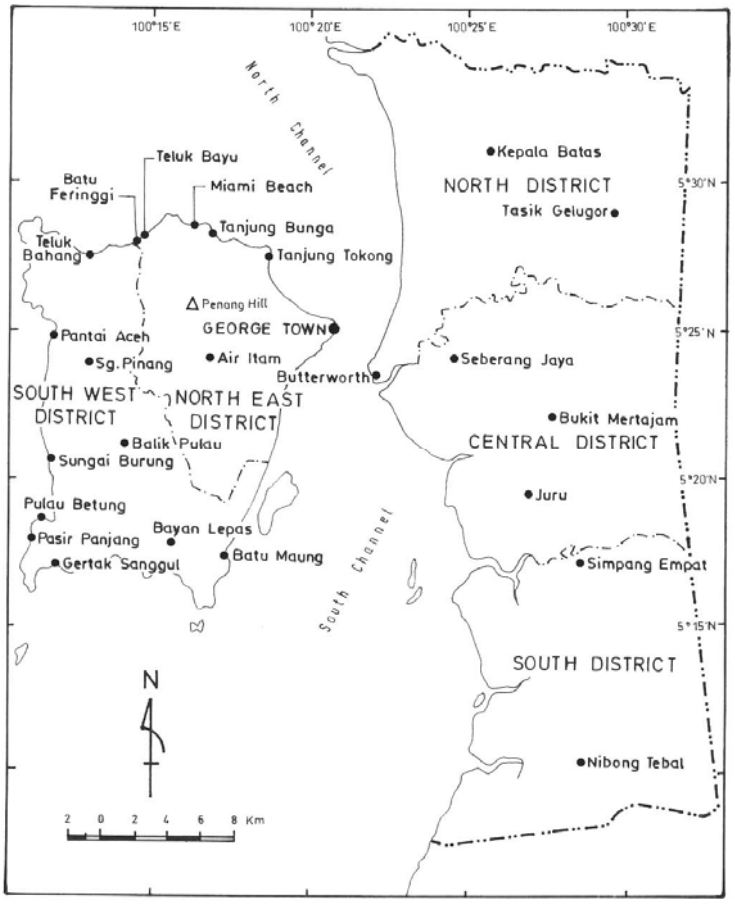

Figure 1. Map of Penang State in Malaysia (mainland and Island) including the names of locations of our interest.

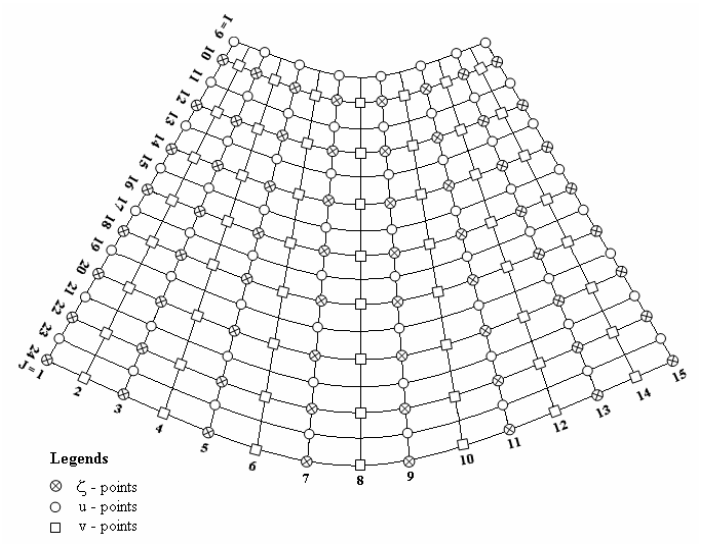

Figure 2. A typical staggered grid system that is used in the numerical scheme where *i* varies from 9 to 24 and *j* varies from 1 to 15.

Level	1	2	3	4	5	6	7	8	9	10	11
Z:	-4.5	-4	-3	-2	-1	0	1	2	3	4	5

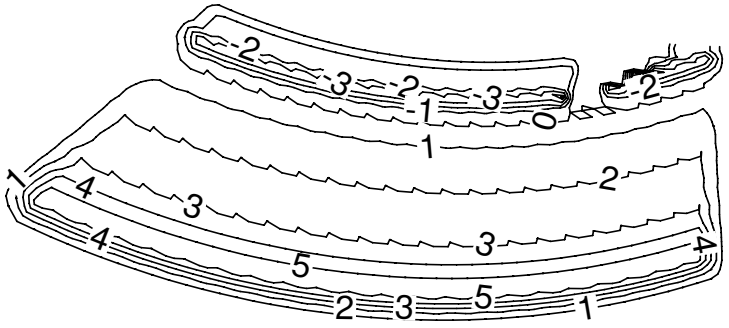

Figure 3. Source of tsunami associated with 26 December 2004 near Sumatra

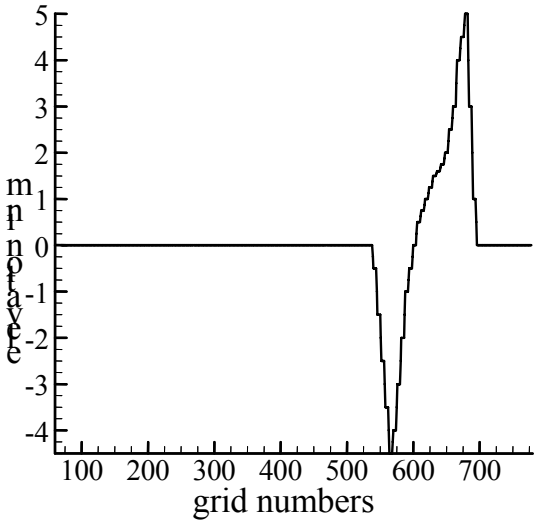

Figure 4. Vertical cross-section of source along the 121st grid line

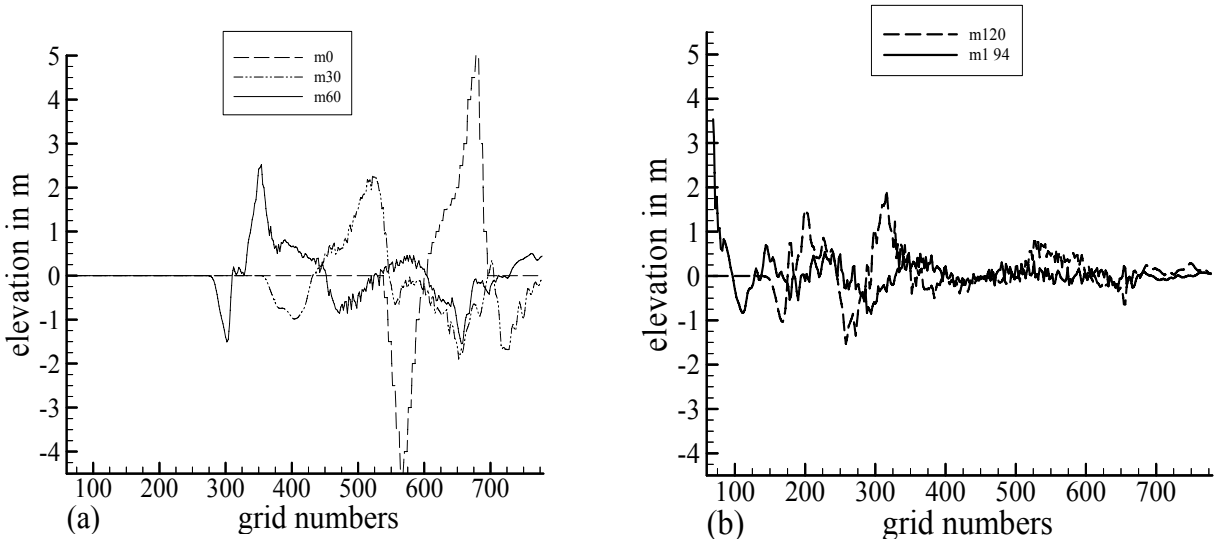

Figure 5. Disturbance pattern at different instants of time along the 121st radial grid line: (a) initial, 30 min, 60 min; (b) 120 min, 194 min

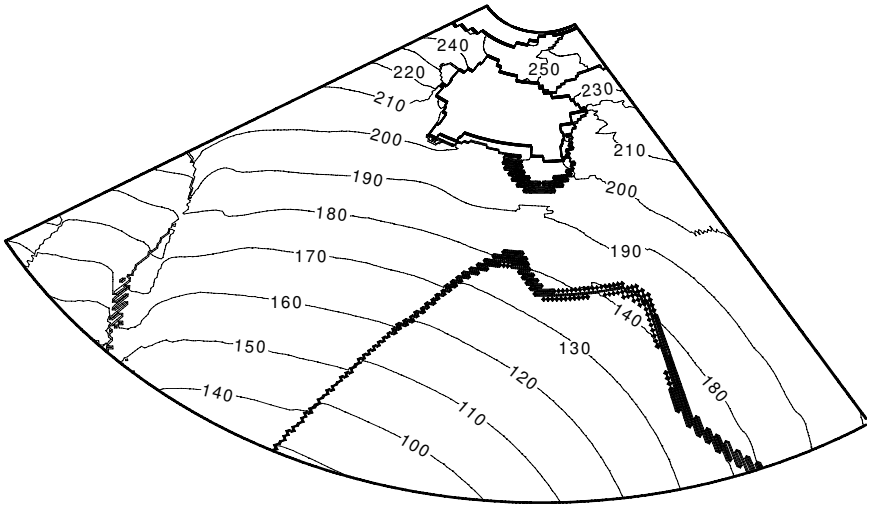

Figure 6. Tsunami propagation time in minutes; the source is within the 10 min contour and Penang Island is at the top. (sea level rise of 0.1 m is considered as the arrival of tsunami)

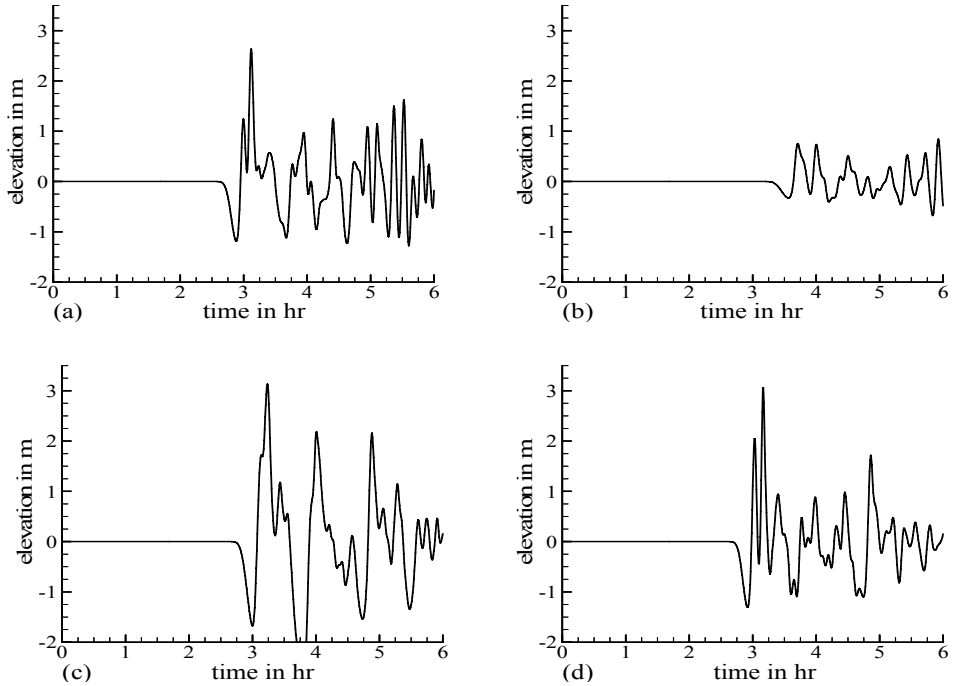

Figure 7. Time histories of computed elevation at coastal locations of Penang Island associated with the tsunami at Sumatra 26 December, 2004 (Subsidence to uplift relative to Malaysian coast): (a) Batu Ferringhi (b) Tanjung Tokong (c) Pantai Aceh (d) Pasir Panjang

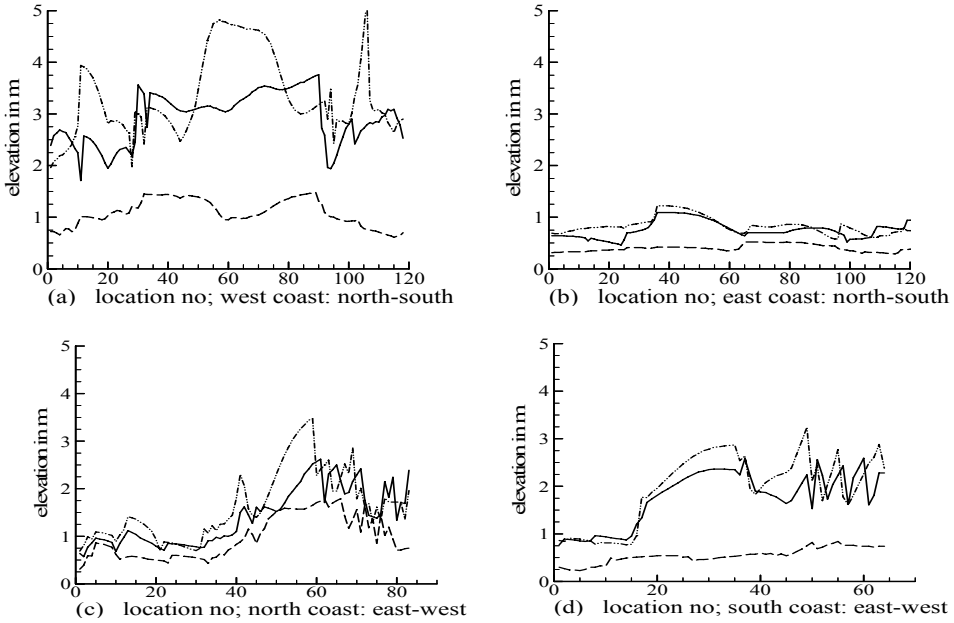

Figure 8. Maximum elevation along the four coasts of the Penang Island: (a) west coast, (b) east coast, (c) north coast and (d) south coast (Solid lines for OS, Dash dot dot lines for CS and long dash for RS)